

Conformational Structure and Dynamics of Arylmethoxyacetates: DNMR Spectroscopy and Aromatic Shielding Effect

Sh. K. Latypov,[†] J. M. Seco, E. Quiñoá, and R. Riguera*

Departamento de Química Orgánica, Facultad de Química, Universidad de Santiago de Compostela, 15706, Santiago de Compostela, Spain

Received August 31, 1994[®]

The ground state conformational geometry and energy of esters of (*R*)- and (*S*)-arylmethoxyacetic acids were evaluated from low temperature ¹H and ¹³C NMR spectra and by means of MM, AM1, and aromatic shielding effect calculations. In solution, the title compounds are constituted by two rotamers in equilibrium. Rotamer ap has the C_α-O and C=O bonds *antiperiplanar* and rotamer sp (lower in energy by 0.4–1.1 kcal/mol) has these bonds *synperiplanar*. In both the ap and the sp the aryl ring is ca. perpendicular to the C=O bond and coplanar with the C_αH bond. Their relative populations and its temperature dependence evaluated by DNMR spectra are in agreement with the stereoselectivity reported for Diels–Alder reactions of dienyl-AMAA esters and support the “perpendicular model” proposed to account for that stereoselectivity. For conformations in which the aryl ring shields the alcohol moiety of the ester, calculated ring current shielding increments compare well with experimental shift values obtained from low-temperature NMR spectra and agree with the conformational model used in the Mislow–Dale–Mosher–Troost method for chiral recognition by NMR.

Introduction

Interest in arylmethoxyacetic acids (AMAA) derives from their use as chiral auxiliaries in Diels–Alder reactions^{1a–d} and for chiral recognition by NMR in the method known as “Mosher method”,^{2a–h} In the former application, stereoselective control is achieved by esterifying dienols with chiral AMAAs, while in the latter case the absolute stereochemistry of chiral alcohols and amines is assigned by reacting them with the (*R*)- and (*S*)-AMAA and comparing the ¹H NMR spectra of the diastereomeric products. In both these applications, the ground state geometry and energies of the ester and amide derivatives play a crucial role. However, to our knowledge no experimental studies of the solution phase conformational equilibria of AMAA esters and the corresponding thermodynamic parameters have been reported.

The idea that the AMAA moiety induces asymmetry in Diels–Alder reactions via an aryl–diene π -stacking interaction^{1a} has recently been discredited due to the observation that nonaromatic dienyl esters are equally effective chiral auxiliaries.^{1b} Instead, a “perpendicular model” has been put forward in which the C_α-OMe bond and the C=O are *syn*, the diene is in the same plane as the carbonyl group, and the aryl ring is perpendicular to

this plane; this latter group thus blocks the approach of the dienophile from one side of the diene.^{1b,d} More recently, *ab initio* calculations have led to the suggestion that in the transition state the conformation of the AMAA moiety resembles the preferred ground state conformation of α -methoxy esters.^{1c}

In the model² proposed to explain the NMR spectra of secondary *O*-methylmandelates, a preferred conformation is assumed in which certain groups of the alcohol moiety are either shielded or nonshielded according to their location in the anisotropic magnetic field around the aryl ring. The validity of this empirical model for chiral recognition has been verified for many compounds of known absolute stereochemistry, but even so, it is not infallible.^{3a–d} Moreover, the real value of the “Mosher method” is in the assignment of the absolute stereochemistry of novel, structurally complex compounds which are isolated in very small quantities; in such cases, configuration assignment cannot be easily subjected to another independent proof.

In this paper we present experimental evidence, drawn from ¹H and ¹³C spectroscopic studies of (–)-menthyl, *tert*-butyl, and isopropyl esters of (*R*)- and (*S*)-AMAA (1–6, Figure 1), in support of calculated molecular geometries and relative energies of the conformers participating in solution equilibria. Conformer geometries and relative energies were obtained by MM and AM1 calculations, respectively; results were corroborated by calculation of ring current shielding increments, which compared well with experimental values.

Calculations

Initial geometries of the (–)-menthyl esters 1–4 with (*R*) or (*S*) configuration at C_α (hereinafter referred to as

[†] On leave from The Institute of Organic & Physical Chemistry of Russian Academy of Sciences, Kazan, 420083, Tatarstan, the Russian Federation.

[®] Abstract published in *Advance ACS Abstracts*, January 1, 1995.

(1) (a) Trost, B. M.; O’Krongly, D.; Belletire, J. L. *J. Am. Chem. Soc.* **1980**, *102*, 7595–7596. (b) Siegel, C.; Thornton, E. R. *Tetrahedron Lett.* **1988**, *29*(41), 5225–5228. (c) Tucker, J. A.; Houk, K. N.; Trost, B. M. *J. Am. Chem. Soc.* **1990**, *112*, 5465–5471. (d) Tripathy, R.; Carroll, P. J.; Thornton, E. R. *J. Am. Chem. Soc.* **1991**, *113*, 7630–7640 and references cited therein.

(2) (a) Actually, several groups have made remarkable contributions to develop this NMR method. See the following references. (b) Raban, M.; Mislow, K. *Tetrahedron Lett.* **1965**, *48*, 4249–4253. (c) Raban, M.; Mislow, K. *Top. Stereochem.* **1967**, *2*, 199–230. (d) Dale, J. A.; Mosher, H. S. *J. Am. Chem. Soc.* **1968**, *90*, 3732–3738. (e) Dale, J. A.; Mosher, H. S. *J. Am. Chem. Soc.* **1973**, *95*, 512–519. (f) Dale, J. A.; Dull, D. L.; Mosher, H. S. *J. Org. Chem.* **1969**, *34*, 2543–2549. (g) Sullivan, G. R.; Dale, J. A.; Mosher, H. S. *J. Org. Chem.* **1973**, *38*, 2143–2147. (h) Trost, B. M.; Belletire, J. L.; Godleski, S.; McDougal, P. G.; Balkovec, J. M. *J. Org. Chem.* **1986**, *51*, 2370–2374.

(3) (a) Kusumi, T.; Fujita, Yo.; Ohtani, I.; Kakisawa, H. *Tetrahedron Lett.* **1991**, *32*(25), 2923–2926. (b) Ohtani, I.; Kusumi, T.; Kashman, Yo.; Kakisawa, H. *J. Org. Chem.* **1991**, *56*, 1296–1298. (c) Ohtani, I.; Kusumi, T.; Kashman, Yo.; Kakisawa, H. *J. Am. Chem. Soc.* **1991**, *113*, 4092–4096. (d) Rieser, M. J.; Hui, Yu.; Rupprecht, J. K.; Kozlowski, J. F.; Wood, K. V.; McLaughlin, J. L.; Hanson, P. R.; Zhuang, Z.; Hoye, Th. R. *J. Am. Chem. Soc.* **1992**, *114*, 10203–10213.

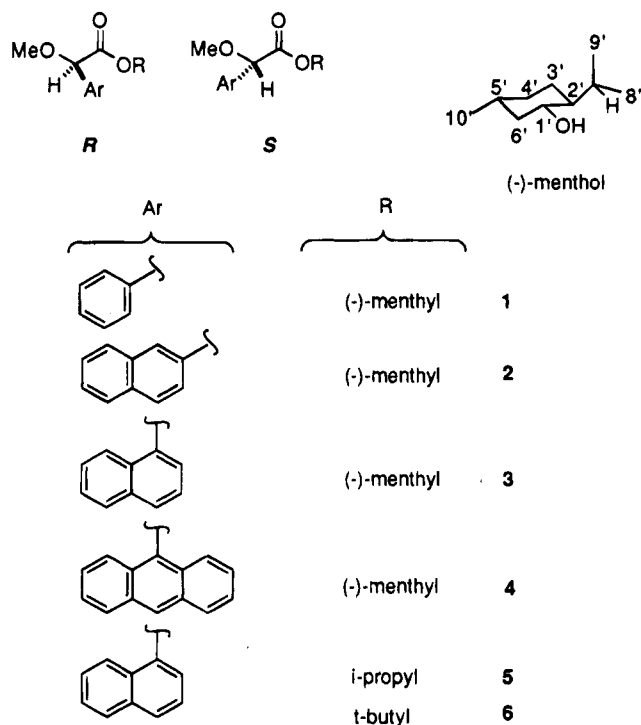


Figure 1.

(*R*)-1 and (*S*)-1 etc.) were obtained by screening of the sterically allowed conformations around the C_α-OMe, C_α-CO, CO-O, and O-C(1') bonds. The energies of suitable rotamers were minimized by molecular mechanics (MM) optimization of their conformations, and those rotamers with energies within 7 kcal/mol of that of the corresponding equilibrium rotamer were selected.⁴ For (*R*)-3 and (*S*)-3, additional conformations obtained by rotation of the C(2')-C(7') and Ar-C_α bonds were also considered.

According to our MM calculations, the rotamers that have most influence on the conformational equilibria of 1-4 are those obtained by rotation around the C_α-CO and C_α-OMe bonds and in the esters with nonsymmetrically substituted aryl rings (2 and 3) and those around the Ar-C_α bond (Figure 2). The potential energy profiles for rotation around C_α-CO have two energy minima: one at which the torsion angles between C_α-OMe and C=O bonds are ca. 15-30° (*synperiplanar*, *sp*, Figure 2a) and another at which these angles are ca. 130-140° (*anti-periplanar*, *ap*, Figure 2b). The energy barrier to rotation around the C_α-CO bond is 3.3 kcal/mol for 1 but increases if the phenyl is replaced by a bulkier aryl ring (3.7, 6.6, or 5.0 kcal/mol for 2-naphthyl, 1-naphthyl, or 9-anthryl, respectively).

The potential energy profile for the C_α-OMe bond predicts three stable rotamers separated by low barriers

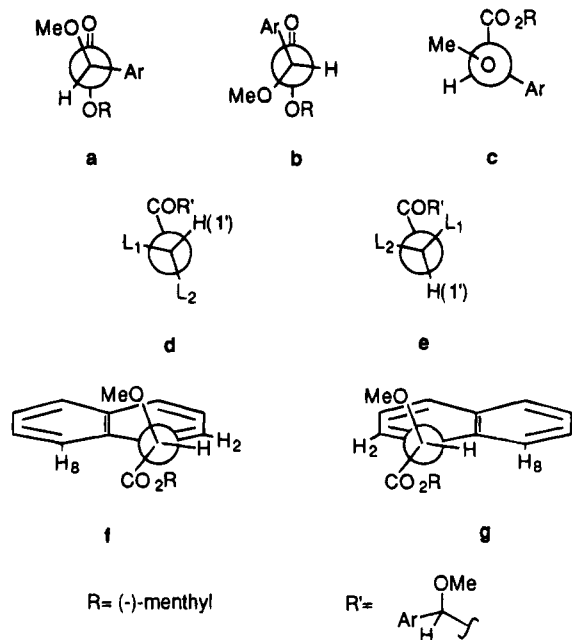


Figure 2. Energy-minimized conformations of the chiral arylmethoxyacetic acid moiety of the esters. Newman projections along the (a and b) C_α-CO bond, (c) C_α-OMe bond, (d and e) O-C(1') bonds, and (f and g) C_α-Ar bonds (only in compounds with non-symmetrically substituted aryl rings).

to rotation of ca. 1.5-2.0 kcal/mol. The equilibrium rotamer has the methoxy methyl group *anti* to the aryl group and *gauche* to the carbonyl group (Figure 2c). The CO-O bond is *gauche* to the C(1')-H, the *anti* orientation being higher in energy by ca. 6.8 kcal/mol (Figure 2d and e, respectively). Finally, the equilibrium conformation predicted for the Ar-C_α bond has the aryl ring and C_αH bond almost planar in all the esters, except those with a nonsymmetrically substituted naphthyl group (2, 3, 5, and 6), for which both *anti* (the lower energy orientation) and *syn* orientations of the naphthyl-H(8) with respect to the C_αH bond are possible (Figures 2f and 2g, respectively). Not unexpectedly, the barrier to rotation around Ar-C_α increases markedly when phenyl is replaced by a bulkier aryl ring (4.0, 4.7, 11.0, or 17.0 kcal/mol for phenyl, 2-naphthyl, 1-naphthyl, or 9-anthryl, respectively).

Optimization of the conformations around the above bonds in isopropyl and *tert*-butyl esters of the 1-naphthyl derivative (5 and 6) produced conformations very similar to those of the (-)-menthyl esters, suggesting that the nature of the esterified alcohol has little influence on conformational equilibria within the acid moiety.

Molecular dynamics simulations of structures 1-6 yielded no additional geometries, thus confirming that the MM calculations had generated all feasible low energy conformations of the acid moiety.

The suitability of molecular mechanics for calculation of molecular geometries is confirmed by the good agreement between the equilibrium geometry calculated for the acid moiety of esters 1-4 and X-ray diffraction studies of *O*-methylmandelates.^{2h} However, MM cannot reliably calculate the energies of conformers, which were therefore obtained by the semiempirical AM1 approach. The conformational geometries resulting from these calculations are close to those obtained by MM, and the relative conformational energies confirm that the *sp* rotamers (around C_α-CO) of compounds 1-6 are more

(4) Details of the calculations are available on request.

(5) (a) Waugh, J. S.; Fessenden, R. W. *J. Am. Chem. Soc.* **1957**, *79*, 846-849. (b) Johnson, C. E.; Bovey, F. A. *J. Chem. Phys.* **1958**, *29*, 1012-1014. (c) Jonathan, N.; Gordon, S.; Dailey, B. P. *J. Chem. Phys.* **1962**, *36*, 2443-2448. (d) Barfield, M.; Grant, D. M.; Ikenberry, D. *J. Am. Chem. Soc.* **1975**, *97*, 6956-6961. (e) Agarwal, A.; Barnes, J. A.; Fletcher, J. L.; McGlinchey, M. J.; Saver, B. G. *Can. J. Chem.*, **1977**, *55*, 2575-2581. (f) Haigh, C. W.; Mallion, R. B. *Progress in NMR Spectroscopy*; Pergamon Press, Ltd.: New York, 1980; Vol. 13, pp 303-344.

(6) (a) Haigh, C. W.; Mallion, R. B. *Mol. Phys.* **1971**, *22*, 955-970. (b) Haigh, C. W.; Mallion, R. B. *Org. Magn. Reson.* **1972**, *4*, 203-228. (c) Dailey, B. P. *J. Chem. Phys.* **1964**, *41*, 2304-2310. (d) Musher, J. *J. Chem. Phys.* **1965**, *43*, 4081-4083.

Table 1. Selected ^1H NMR Chemical Shift Data^a (ppm, TMS as Internal Reference) of Esters 1–6 (Atom Numbering Is as in Figure 1). All Spectra Were Recorded in 4:1, $\text{CS}_2/\text{CD}_2\text{Cl}_2$

compound	<i>T</i> , K	conformation	H(7')	Me(8')	Me(9')	Me(10')	C_αH	OMe
menthol	296		2.097	0.899	0.768	0.890		
(<i>R</i>)-1	296		1.25	0.651	0.418	0.888	4.533	3.301
(<i>R</i>)-1	153		ca. 0.7	0.561	0.165	0.898	4.641	3.284
(<i>S</i>)-1	296		1.7	0.846	0.642	0.822	4.567	3.307
(<i>S</i>)-1	153		1.87	0.895	0.681	0.795	4.636	3.257
(<i>R</i>)-2	296		ca. 1.2	0.532	0.345	0.878	4.715	3.358
(<i>R</i>)-2	153		ca. 0.52	0.448	0.127	0.891	4.815	3.324
(<i>S</i>)-2	296		1.75	0.801	0.631	0.815	4.731	3.358
(<i>S</i>)-2	153		ca. 1.8	0.892	0.711	0.711	4.815	3.298
(<i>R</i>)-3	298		0.72	0.32	0.09	0.839	5.12	3.300
(<i>R</i>)-3	153	A, 69%	-0.166	0.158	-0.476	0.852	4.981	3.253
(<i>R</i>)-3	153	B, 17%	0.9	0.406	0.327		5.494	3.446
(<i>R</i>)-3	153	C, 14%	ca. 2	0.9	0.768			3.2–3.1
(<i>S</i>)-3	296		1.65	0.782	0.596	0.780	5.176	3.365
(<i>S</i>)-3	153	A, 75%	1.8	0.888	0.711	0.711	4.952	3.138
(<i>S</i>)-3	153	B, 25%			0.078	0.078	5.497	3.401
(<i>R</i>)-4	296		0.085	0.047	-0.118	0.847	6.050	3.396
(<i>R</i>)-4	163		-0.384	-0.05	-0.249	0.738	6.07	3.2
(<i>S</i>)-4	296		1.8	0.834	0.732	0.658	6.047	3.318
(<i>S</i>)-4	153		1.823	0.759	0.651	0.583	6.102	3.027
			H(1')	Me	Me			
5	296		4.881	1.16	0.989		5.158	3.362
	153	4, 33%		1.094	0.73		4.922	2.95
	153	3, 30%		1.183	0.88		5.482	3.171
	153	2, 22%	4.79	1.183	1.		5.371	3.264
	153	1, 15%	4.88	1.262	0.945		5.1	3.422
				t-Bu				
6	296			1.289			5.115	3.366
	153	1, 41%		1.275			4.886	3.144
	153	2, 32%		1.361			5.232	3.332
	153	3, 16%		1.246			5.382	3.199
	153	4, 11%		1.159			4.819	3.037

^a Digital resolution = 0.16 Hz.

stable than the *ap* rotamers (by 0.6–1 kcal/mol), in keeping with *ab initio* calculations^{1c} and our own preliminary experimental results.⁷

An important conformational feature derived from the MM calculations is the approximately perpendicular arrangement of the aryl ring and the carbonyl group in compounds 1–6 ($\text{Ar}-\text{C}_\alpha\text{C}=\text{O}$ dihedral angle ranges from 99 to 110°). Thus, the *sp* rotamers of the (*R*)-esters and the *ap* rotamers of the (*S*)-esters will have Me(8') and Me(9') within the positively shielding region around the aryl ring.^{5,6}

Because the energies of the *sp* and *ap* rotamers are close, the equilibrium between them should be significantly altered by temperature changes; these shifts in equilibrium can be followed by ^1H and ^{13}C NMR spectroscopy, monitoring the time-averaged chemical shifts of the shielded and nonshielded methyl protons. Moreover, if the rate of rotamer interconversion is slow on the NMR time scale, it may be possible to distinguish conformers in which the menthyl isopropyl groups are shielded from those in which they are not. The conformational equilibria of these esters could thus be probed, and the thermodynamic parameters describing these equilibria established. It should also be possible to quantitatively correlate shielding effects with the geometric parameters of the individual conformers.

NMR Results

In the room temperature ^1H NMR spectra of compounds 1–4, Me(8') and Me(9') signals are shielded (with

respect to (-)-menthol) in both (*R*)- and (*S*)-menthyl esters (Table 1 and Figure 3). Thus, for both diastereoisomers there exists a conformation (or set of conformations) in which these methyl groups sit just above/below the plane of the aryl ring. The extent to which these methyls are shielded in esters 1–4 can be correlated with the absolute configuration at C_α and the nature of the aryl ring: shielding of Me(8') and Me(9') was greater in the (*R*) esters than in the (*S*) esters; these shielding effects were two-to-three times greater in esters of AMAAs with naphthyl or anthryl rings (2–4) than in the phenyl derivative 1 (see Table 1).

The effects of varying the probe temperature (*T*) were significant, just as our calculations had suggested. Changes in the appearance and shift of the Me(8'), Me(9'), and Me(10') signals can be correlated with the absolute configuration at C_α ; the Me(8') and Me(9') signals of (*R*)-esters were shielded upon decreasing *T*, while those of the corresponding (*S*)-esters were not shielded;⁸ the Me(10') signal showed the opposite behavior, i.e., it was not shielded in the (*R*)-esters and shielded in the (*S*)-esters upon decreasing *T* (Figure 4).

The influence of the aryl ring was manifest in the increase in the aromatic shielding effect, which was greatest for naphthyl derivatives 2 and 3, smallest for the 9-anthryl derivative 4, and had an intermediate value for the phenyl derivative 1.

(7) Seco, J. M.; Latypov, Sh.K.; Quiñoá, E.; Riguera, R. *Tetrahedron Lett.* 1994, 35(18), 2921–2924.

(8) In both (*R*)-4 and (*S*)-4, C(7'-9') signals were shifted slightly upfield and showed some evidence of slow exchange, although this exchange was not characteristic of an equilibrium between conformers with Me(8') and Me(9') shielded and nonshielded. These effects were later attributed to changes in the relative population of the $\text{C}_\alpha\text{-OMe}$ rotamers (see Discussion).

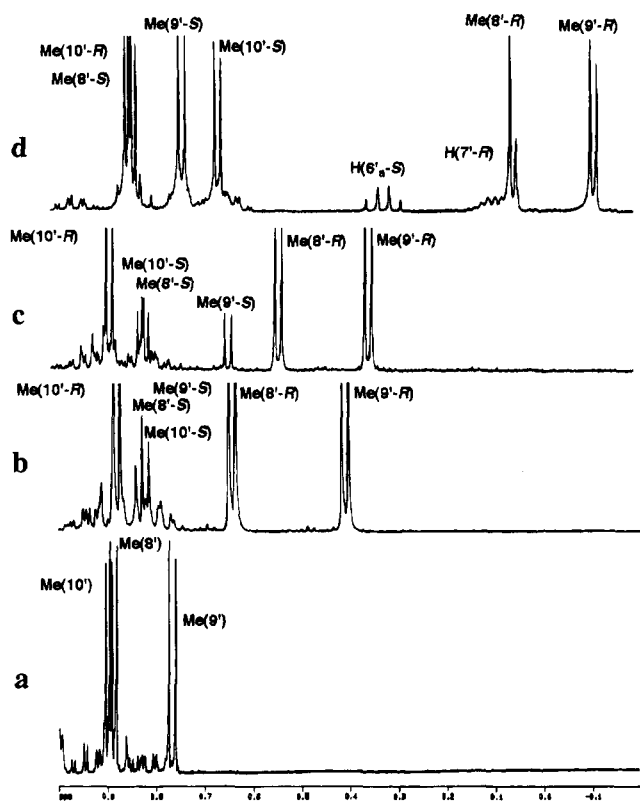


Figure 3. Partial ^1H NMR spectra of (-)-menthol and (-)-menthyl esters of (*R*)- and (*S*)-arylmethoxyacetic acids in 4:1 $\text{CS}_2/\text{CD}_2\text{Cl}_2$ at 298 K: (a) (-)-menthol; (b) Ar = Ph, (*R*)-**1** and (*S*)-**1**; (c) Ar = 2-naphthyl, (*R*)-**2** and (*S*)-**2**; (d) Ar = 9-anthryl, (*R*)-**4** and (*S*)-**4**.

The low temperature NMR spectra of 1-naphthyl derivatives (*R*)-**3** and (*S*)-**3** are particularly interesting. In the ^1H NMR spectra of (*R*)-**3** there is evidence of two dynamic processes, one of which proceeds twice as fast as the other. Between 193 and 173 K the signals due to C_αH , MeO, and ArH of the acid moiety broadened, and between 173 and 168 K the doublets due to Me(8') and Me(9') of the menthol moiety coalesced, becoming two broad humps with unequal intensities. At ca. 168 K the C_αH signal appeared as two sharp lines of unequal intensity, indicating that a chemical exchange process is affecting this signal. Line shape analysis (between 183 and 178 K) confirmed that chemical exchange was occurring and established that it was mainly affecting the local magnetic environments of C_αH , MeO, and ArH of the acid moiety.

At 163 K the Me(8') and Me(9') signals began to sharpen, and those due to C_αH and OMe broadened slightly, together indicating that there was a second dynamic process. This was confirmed by the spectrum recorded at 153 K, in which the appearance of all signals was indicative of slow chemical exchange (Figure 4). Line shape analysis (between 178 and 163 K) established that this process mainly affects the local magnetic environment of Me(8') and Me(9') of the menthyl moiety, while only very slightly altering that of C_αH and OMe of the acid. Comparison of the results of line shape analysis indicated that chemical exchange is twice as fast for the low-temperature process (173–168 K); this was confirmed by examination of the simpler DNMR spectra of compounds **5** and **6** (lacking signals due to the menthyl group).

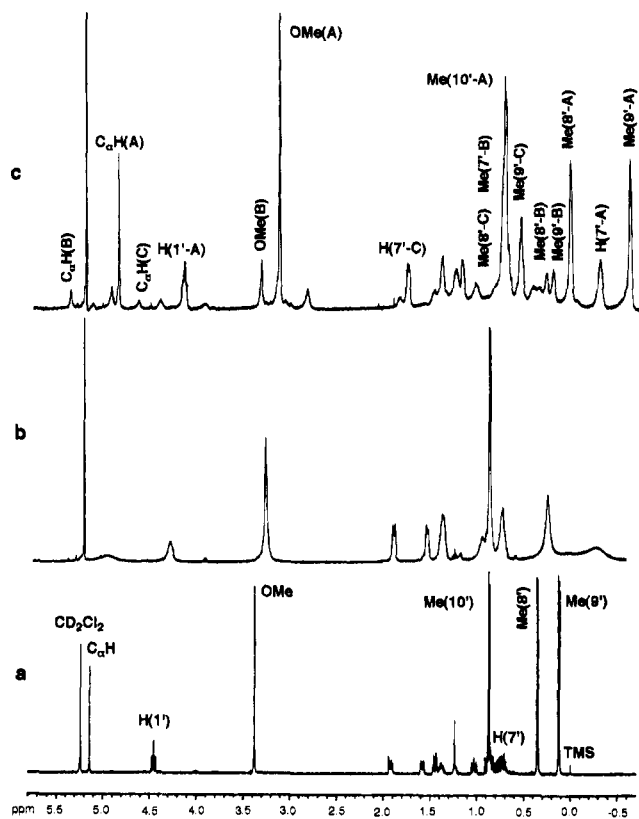


Figure 4. Partial ^1H NMR spectra of the (-)-menthyl ester of (*R*)-**3** in 4:1 $\text{CS}_2/\text{CD}_2\text{Cl}_2$ at (a) 298 K, (b) 183 K, and (c) 153 K.

At 153 K, the ^1H NMR spectrum of (*R*)-**3** shows signals corresponding to three components (designated A, B, and C; Figure 4c). These signals were fully assigned by means of 2D COSY experiments: for example, Me(8') and Me(9'), respectively, appear as broadened doublets at -0.476 and 0.158 (major component, A), 0.327 and 0.406 (B), and 0.77 and 0.95 ppm (C). The signals due to H(7') of the A, B, and C components, some of which were overlapped in the 1D spectra, were located in the 2D spectra: their chemical shifts and appearance were similar to those of the methyl signals, in keeping with the proximity of H(7') to Me(8') and Me(9') in the molecular structure.

Low-temperature NOESY experiments demonstrated that the three sets of signals are derived from species in equilibrium (Figure 5): exchange cross peaks were observed between the Me(9') and Me(8') signals of components A and B and components B and C; in the signals due to individual components, cross-relaxation was observed between Me(9') and H(1'), Me(8') and H(2'), and C_αH and ArH in the major component (A) and between ArH and C_αH in the minor component (B). The peaks due to the C component were of very low intensity and overlapped in some cases, so no useful information could be gleaned from these signals, even in the 2D spectra.

In the ^1H NMR spectra of the (*S*) diastereoisomer of **3**, the ArH, MeO, and C_αH signals began to broaden at ca. 183 K, again indicating slow chemical exchange at that temperature, but the signals due to the menthyl isopropyl group did not coalesce, even at 156 K. However, the appearance and chemical shifts of the ArH, MeO, and C_αH signals in the low-temperature spectra closely corresponded to those of the A and B components of (*R*)-**3**

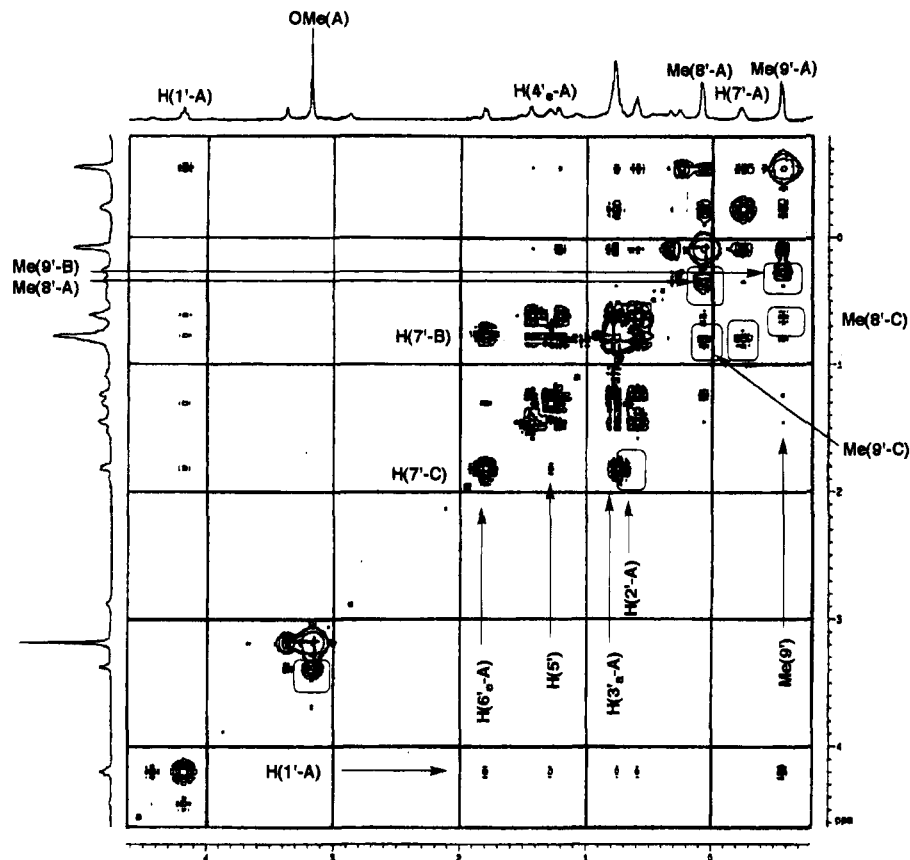


Figure 5. Partial 2D ^1H NOESY spectrum of compound (*R*)-**3** at 153 K (cross-relaxation peaks enclosed in a frame are due to chemical exchange).

at 153 K, suggesting that the (*R*)-**3** and (*S*)-**3** diastereoisomers are involved in similar equilibria, even though the population of the C conformer is apparently much lower for (*S*)-**3**.

In the ^{13}C NMR spectra of (*R*)-**3**, the signals due to C_α and OMe of the acid moiety and $\text{C}(6')$ of the menthyl moiety began to broaden at 193 K. At 183 K a two-component spectrum is obtained (peaks with unequal intensities at 83.2 and 77.5 ppm for C_α and broadened peaks for $\text{C}(7')$, $\text{C}(8')$, and $\text{C}(9')$,⁹ and at 173 K a three-component spectrum is observed. These changes confirm the findings of the ^1H DNMR studies, i.e., that two chemical exchange processes are occurring in this molecule. Comparison of the spectra obtained at each temperature confirmed that the slower process mainly affects the C_α carbon (the chiral center), while the faster process mainly affects $\text{C}(7')$, $\text{C}(8')$, and $\text{C}(9')$ of the menthyl moiety.

The ^1H NMR spectra of compounds **1**, **2**, and **4** showed no sign of the "slow" dynamic process seen in (*R*)-**3**. Me-(8') and Me(9') of the phenyl derivatives (*R*)-**1** and (*R*)-**2** and to a lesser extent those of the 9-anthryl derivatives (*R*)-**4** and (*S*)-**4** were all shielded⁸ as the probe temperature was decreased, but no coalescence was observed even at 153 K. The signals due to H(1) and H(8) of (*R*)-**4** and (*S*)-**4** are broadened between 243 and 233 K. One of those two signals moved, in the temperature range 233–153 K, 0.22 ppm upfield from the other. The low-temperature 2D NOESY revealed cross peaks between C_αH and the

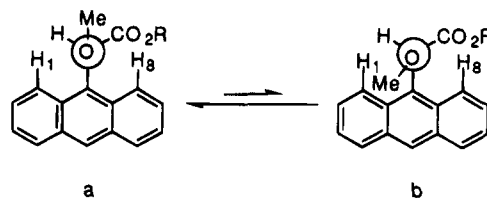


Figure 6. Low energy rotamers around the $\text{C}_\alpha\text{-OMe}$ bond in (*R*)- α -methoxy- α -(9-anthryl)acetates.

signal that remains unmoved ($\delta = 8.36$ ppm at 193–223 K), which is therefore assigned to the aryl proton (designated H(8), Figure 6), *synperiplanar* to C_αH , and close enough to interact via a dipole–dipole mechanism. The signal moving upfield ($\delta = 8.32$ ppm at 173 K) is thus due to H(1) *antiperiplanar* to C_αH .

The possibility that the $\text{O-C}(1')$ bond may have been involved in that exchange process was ruled out because the ^1H NMR spectra of isopropyl and *tert*-butyl esters **5** and **6** showed the same two dynamic processes already seen at 183 and 163 K in (*R*)-**3**. At 153 K, most protons reflect the presence of four conformers in equilibrium. Thus, in the case of **6**, the *tert*-butyl group produces a four-line pattern and not six as would be expected if rotation around the $\text{O-C}(1')$ bond were slow at this temperature.

Discussion

Our calculations and DNMR spectroscopy studies suggest that esters **1–6** exist in solution as at least two pairs of rotamers in equilibrium, one of which is shown for the (–)-menthyl esters of (*R*)- and (*S*)- α -methoxy- α -

(9) Menthyl signals in the NMR spectra were assigned by means of (^1H – ^{13}C) DEPT and (^1H) HMQC experiments and with reference to 2D COSY and 2D NOESY spectra, and *Prog. Chem. Org. Nat. Prod.* **1979**, 36.

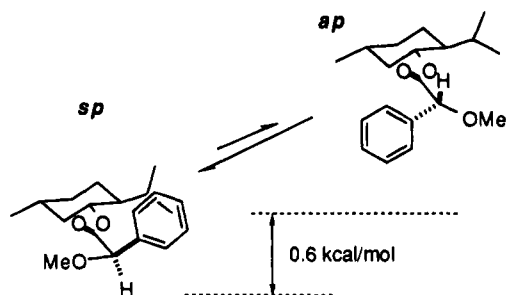


Figure 7. Equilibrium between the *sp* (shielded) and *ap* (nonshielded) rotamers around the C_{α} -CO bond of (*R*)-1. Energy calculated by AM1.

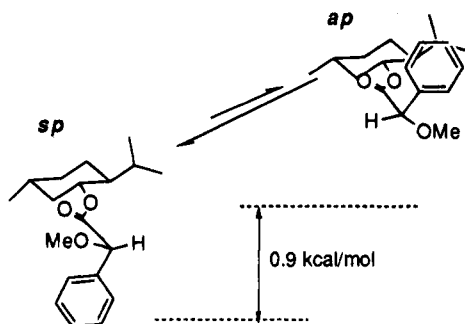


Figure 8. Equilibrium between the *sp* (nonshielded) and *ap* (shielded) rotamers around the C_{α} -CO bond of (*S*)-1. Energy calculated by AM1.

phenylacetic acid ((*R*)-1 and (*S*)-1) in Figures 7 and 8, respectively.

The more stable *sp* rotamer of the (*R*) derivatives has the isopropyl group of the menthyl moiety within the positively shielded region of the aryl ring; the ^1H and ^{13}C NMR signals due to this group are therefore shifted upfield relative to those of the isopropyl in (–)-menthol (this is identified as the shielded conformation, SC).

The opposite occurs for (*S*) isomers: the *sp* rotamer is again the more stable, but in this conformation the isopropyl group is not shielded (denominated the non-shielded conformation, NSC). Since the chemical shifts of the Me(8') and Me(9') will be time-averaged, it is the relative population of the *sp* and *ap* conformations of each diastereoisomer that determine the magnitude of the upfield shift; this shift is therefore greater for the (*R*) isomers (for which the SC is more stable) than for the (*S*) isomers (for which the NSC is more stable).

In solutions of esters with nonsymmetrically substituted aryl rings, the conformational equilibria are more complex (Figures 4 and 5). The cross peaks observed in the 2D NOESY experiments confirm that (*R*)-3 exists in at least three conformations, each one giving rise to a different set of NMR data (the A, B, and C components observed may contain time-averaged contributions from other conformations). In keeping with the greater stability of the SC in the (*R*) esters, the most intense peaks due to Me(8') and Me(9') are the most shielded (component A), while the less intense peaks are those that are only slightly shielded (component B) or not shielded at all (component C).

DNMR spectroscopy indicates that the two dynamic processes occurring in solution lead to changes in the local magnetic environment of different parts of the molecule. The slower process mainly affects the $C_{\alpha}\text{H}$ signal, which shows evidence of slow exchange at ca. 183

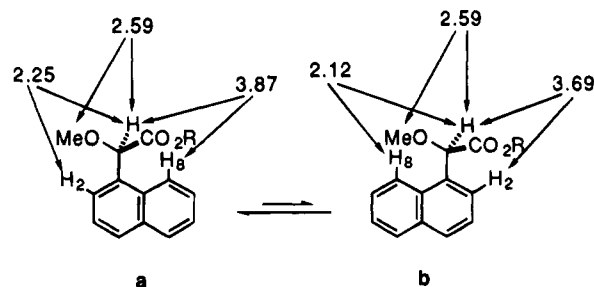


Figure 9. Low energy rotamers around the $\text{Ar}-C_{\alpha}$ bond in (*R*)-3. Proton-proton distances are in Å.

K, not only in (*R*)-3 and (*S*)-3 but also in 5–6. Thus, neither the stereochemistry at C_{α} nor the nature of the alcohol moiety has much influence on the slower dynamic process. Since the signals due to the naphthyl protons are also affected at 183 K, the conformational change occurring should involve rotation around the $\text{Ar}-C_{\alpha}$ bond. This was confirmed by examination of the in-plane paramagnetic deshielding effects of the aryl ring^{5,6} on $C_{\alpha}\text{H}$, by the existence of NOE¹⁰ between ArH and $C_{\alpha}\text{H}$, and by ^{13}C NMR data¹¹ as follows.

For 1-naphthyl derivatives, Figure 9 shows the low energy orientations of the naphthyl ring that were predicted by MM calculations (see also Figures 2f and 2g). In the *anti* **a** rotamer (Figure 9a), $C_{\alpha}\text{H}$ should experience less deshielding by the naphthyl ring than in the *syn* **b** rotamer (Figure 9b); in the ^1H DNMR spectra of (*R*)-3 (173–178 K), the peaks due to $C_{\alpha}\text{H}$ at 4.981 and 5.494 ppm (relative intensities 4:1) can thus be assigned to the **a** and **b** rotamers, respectively (and similarly for (*S*)-3).

The low-temperature 2D COSY and NOESY of (*R*)-3 confirm the above assignments: In the major rotamer (**a**) there is long-range coupling between $C_{\alpha}\text{H}$ and H(8)¹² and NOE between $C_{\alpha}\text{H}$ and H(2) and, to a lesser extent, between $C_{\alpha}\text{H}$ and H(8) (component A). For the minor rotamer (**b**), there is no long-range coupling between $C_{\alpha}\text{H}$ and H(8), and NOE is only observed between $C_{\alpha}\text{H}$ and H(8) (component B). MM calculations for the major and minor rotamers, respectively, yield $C_{\alpha}\text{H}-\text{H}(2)$ and $C_{\alpha}\text{H}-\text{H}(8)$ distances that are short enough to account for the observed NOEs. Similarly, the geometrical arrangement of the $C_{\alpha}\text{H}$ and H(8) protons in the major component is in good agreement with the long-range coupling observed (Figure 9).

The low-temperature 2D NOESY spectra of (*R*)-3 also show NOE between OMe and $C_{\alpha}\text{H}$ and OMe and H(8), in accordance with the calculations predicting a preferred rotamer around the $C_{\alpha}-\text{OMe}$ bond (Figure 2c).

For its part, the ^{13}C NMR spectrum of (*R*)-3 shows the C_{α} signal markedly altered by temperature changes: at 183 K the signal due to rotamer **b** resonates 6 ppm upfield to that of rotamer **a**, as a result of steric interactions between $C_{\alpha}\text{H}$ and H(8) in **b** (γ effect).¹¹ A similar interaction between $C_{\alpha}\text{H}$ and H(1') could also explain the

(10) Neuhaus, D.; Williamson, M. P. *The nuclear Overhauser effect in structural and conformational analysis*; VCH: New York, 1989.

(11) Breitmaier, E.; Voelter, W. *Carbon-13 NMR Spectroscopy: high resolution methods and applications in organic chemistry and biochemistry*; VCH: Weinheim, 1987.

(12) Gunther, H. *NMR Spectroscopy: an introduction*; John Wiley & Sons: New York, 1987; p 80.

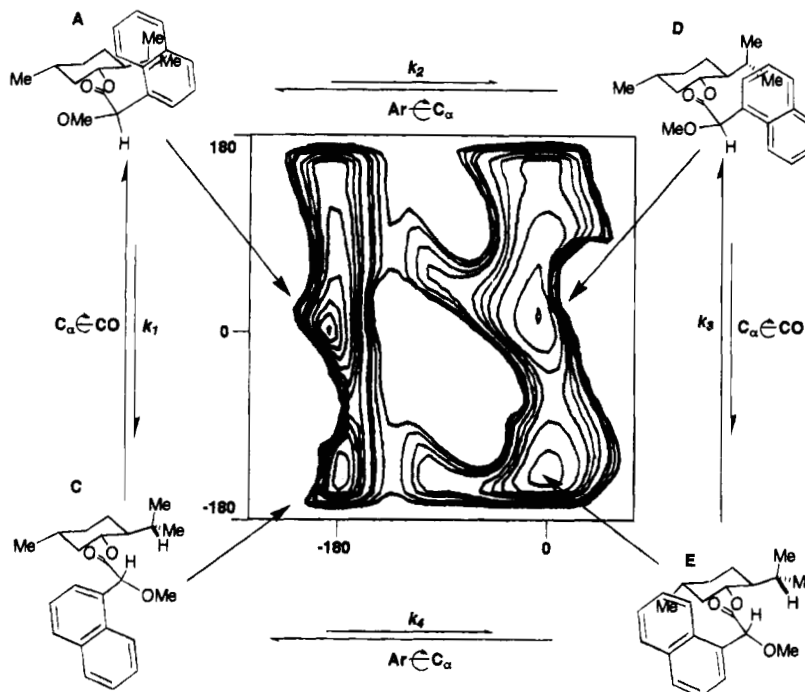


Figure 10. Interconversion path of the main conformers of (-)-menthyl (-)-(*R*)- α -methoxy- α -(1-naphthyl)acetate (*R*-**3**) and contour map of the energy as a function of the C_α -CO and Ar- C_α angles.

shift of C_α -H, but it is ruled out on the basis of previous DNMR studies¹³ and *ab initio* calculations.^{3c}

The above results confirm that the slower chemical exchange process occurring in (*R*)-**3** is rotation around the C_α -Ar bond. Doubling of the C_α H and OMe NMR signals is due to the two low-energy orientations of the naphthyl ring, which, according to MM calculations, are separated by an energy barrier of 11.0 kcal/mol, in good agreement with the value of 12.4 kcal/mol reported¹⁴ for 1-isopropyl-2-methylnaphthalene.

The faster chemical exchange process occurring in (*R*)-**3** is interconversion of the shielded and nonshielded conformers. Our calculations indicate that rotation about the C_α -CO bond is responsible for this process, although the O-CO and/or O-C(1') bonds could also be involved. However, DNMR studies¹³ and *ab initio* calculations^{3c} indicate that in solution the rotamer around the O-CO bond is much more stable with C=O and O-C(1') groups *syn*, ruling out any role for the O-CO bond in the faster exchange process. Rotation around O-C1' can also be eliminated because the *anti* orientation of the CO-O-C(1')-H fragment is higher in energy (6.8 and 1.1 kcal/mol according to MM and AM1, respectively), and moreover, DNMR of the corresponding isopropyl and *tert*-butyl esters **5** and **6** showed no freezing of rotation around this bond at that temperature (153 K). Furthermore, if rotation around O-C1' were involved, a collapse of signals should be observed in the low-temperature NMR spectra of **1**, **2**, and **4** that share the same alcohol part as (*R*)-**3**.

Therefore, this second coalescence of signals observed in (*R*)-**3** is produced by rotation around the C_α -CO bond as suggested by the calculations and represents the way to convert the SC conformer of (*R*)-**3** to the NSC one.

The calculations and spectroscopic studies carried out for (*R*)-**3** lead to the conformational equilibria shown in

Figure 10. Conformers D and E are interconvertible by rotation of the C_α -CO bond; this rotation having the lowest energy barrier is fast on the NMR time scale and its effects are time-averaged, even at low temperatures (see the B component in the ¹H NMR spectrum; Figure 4c). Conformers A and D are interconvertible by rotation around the C_α -Ar bond, as are conformers C and E; in both cases the energy barriers to rotation are higher than for the D/E equilibrium, so rotation is slow on the NMR time scale below room temperature and can be discerned in the C_α H signals (see components A-C; Figure 4c). Conformers A and C are interconvertible by rotation around the C_α -CO bond; the barrier to this rotation is intermediate between those of the D/E and A/D or C/E equilibria, so evidence of this chemical exchange process can be obtained only in the very low temperature NMR of Me(8') and Me(9') (see components A and C; Figure 4c).

The DNMR spectra of (*S*)-**3** showed chemical exchange involving rotation around the Ar- C_α bond only. However, the NMR spectra of (*S*)-**3** and (*R*)-**3** evolve concordantly with decreasing temperature, suggesting that these diastereoisomers are in fact involved in very similar conformational equilibria. The C component is clearly contributing to the time-averaged spectrum of (*S*)-**3** recorded at room temperature, but signals due to this component are not apparent in the low-temperature spectrum; this was either because the concentration of the shielded conformer was too low at lower temperature or due to overlapping of the peaks.

In the ¹H NMR spectra of (*R*) and (*S*) esters **1**, **2** and **4**, changes in the chemical shifts of C_α H and the menthyl isopropyl group suggest that rapid chemical exchange similar to the equilibrium between *sp* and *ap* of (*R*)-**3** is occurring (cf. A/C equilibrium in Figure 10). For both (*R*)-**4** and (*S*)-**4**, the *sp* rotamers (around C_α -CO) are much more stable than the *ap* rotamers, but the conformers obtained by rotation around the C_α -OMe bond (Figures 6a and 6b) are much closer in energy; the

(13) (a) Drakenberg, T.; Forsen, S. *J. Phys. Chem.* **1972**, *76*, 3582-3586. (b) Grindley, T. B. *Tetrahedron Lett.* **1982**, *23*, 1757-1760.

(14) Mannschreck, A.; Ernst, L. *Chem Ber.* **1971**, *104*, 228-247.

populations of the two stable rotamers are therefore significantly altered by temperature changes, which consequently lead to very slight changes in average NMR spectra: the anthryl H(1) signal shifts upfield due to difference of the electric field effect of the polar OMe group;¹⁵ the H(7'), Me(8'), and Me(9') protons are further shielded because the magnetic field gradient of the aryl ring in the region of the isopropyl group is higher in the most stable rotamer (Figure 6a).

Line shape analysis of the DNMR data for (*R*)-**3** yielded^{16,17} a barrier to rotation around the C_α-CO bond of 7.2 kcal/mol, slightly higher than the corresponding values calculated for esters 1-6 by MM (5.0-6.6 kcal/mol). The activation energy for rotation around the C_α-Ar bond was found to be 8.3 kcal/mol. This value is lower than the theoretically calculated one (11.0 kcal/mol by MM). The lack of accurate torsional parameters for α-alkoxy esters^{1c} may account for the low values produced by the MM force-field calculations, although the possibility that steric factors in the transition state induce synergistic rotations around the C_α-CO and C_α-Ar bonds cannot be ruled out.¹⁸

Ring Current Effect in the Shielded Conformers

The stable conformers of compounds 1-4 and the preferred pathways by which they interconvert have been established above by means of MM and DNMR spectroscopy. Starting from these molecular geometries, we examined whether ring-current-effect theory could adequately reproduce the shifts observed in the ¹H NMR spectra.

As far as we know, the ring current increments of the menthyl isopropyl protons in (*R*)-**3** are the largest ever reported for out-of-plane protons (for Me(8'), Me(9'), and H(7'), $\Delta\sigma_{3-R} - \delta_{menthol} = -0.7, 1.2,$ and 2.3 ppm, respectively). The shielding at each of these latter positions can be related to the relative orientations of the affected protons and the naphthyl ring in the SC. The assignment of the signals and the conformation of the isopropyl group predicted by MM (Me(9') and H(2') *trans*) are supported by NOE data confirming the proximity of Me(9') to H(1') and Me(8') to H(2') (the calculated mean distances between these protons are 2.93 and 2.73 Å, respectively). Diamagnetic shielding of the isopropyl protons of SC of (*R*)-**3** was calculated using data obtained by both quantum-mechanical⁶ and semiclassical⁵ methods (Table 2). Calculated shielding increments are practically independent of the rotation around the C_α-OMe bond, but do vary with the conformation around the C_α-Ar bond. The calculated difference between the ring current increments for Me(8') and Me(9') is 0.68 ppm in conformer A and 0.1 ppm in conformer D (Figure 10) in good agreement with the experimental values of 0.5 ppm (conformer A) and 0.05 ppm (exchange average of D and E); conformers A and D correspond to structures **a** and **b** in Figure 9, with C_α-H *antiperiplanar* and *synperiplanar* to Ar-H(8) respectively.

In Figure 11, the experimental ring current increments ($\Delta\sigma = \delta_{3-R} - \delta_{menthol}$) are plotted against values calculated

Table 2. Calculated and Experimental Ring Current Shielding Increments ($\Delta\sigma$ ppm) for the Isopropyl Protons of Esters 1-4 in the Shielded Conformation (Atom Numbering Is as in Figure 1)

compound		protons		
		H(7')	Me(8')	Me(9')
<i>(R)</i> -1	$\Delta\sigma^a$	1.4	0.5	0.75
	$\Delta\sigma^b$	0.5	0.18	0.26
	$\Delta\sigma_{exp}$	≥ 1.4	≥ 0.34	≥ 0.6
<i>(S)</i> -1	$\Delta\sigma^a$	0.8	0.2	0.3
<i>(R)</i> -2	$\Delta\sigma^a$	2.4	0.8	1.2
	$\Delta\sigma_{exp}$	≥ 1.58	≥ 0.45	≥ 0.64
	$\Delta\sigma^c$	2.75	1.1	0.8
<i>(S)</i> -2	$\Delta\sigma^a$	2.5	0.88	1.56
	$\Delta\sigma^c$	2.27	0.8	1.41
	$\Delta\sigma^b$	0.88	0.3	0.53
A conformer	$\Delta\sigma_{exp}$	2.26	0.74	1.24
	$\Delta\sigma^a$	2.25	1	0.88
	$\Delta\sigma^c$	2.04	0.90	0.8
D conformer	$\Delta\sigma^b$	0.77	0.39	0.26
	$\Delta\sigma_{exp}$	1.2	0.49	0.44
	$\Delta\sigma^a$	2.2	0.88	1.3
<i>(S)</i> -3	$\Delta\sigma^a$	3.52	1.4	1.75
<i>(R)</i> -4	$\Delta\sigma^c$	2.9	1.2	1.5
	$\Delta\sigma_{exp}$	≥ 2.45	≥ 0.97	≥ 1.0
	$\Delta\sigma^a$	4	1.54	1.84

^a Calculated from semiclassical data⁵ using $p = 0.918$ benzene radii units (1.28 Å). Ring-current intensity coefficients corrected to 1.1 (naphthyl) or 1.1 and 1.28 (outer and center rings, respectively, of anthryl) benzene ring current intensity units.^{5c}
^b Calculated from quantum-mechanical data.^{6c} ^c Calculated from semiclassical data without correction of ring current intensity coefficients for naphthyl and anthryl derivatives.

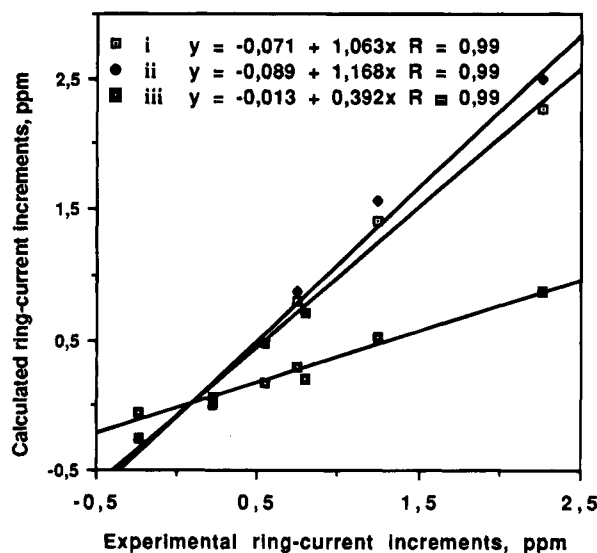


Figure 11. Plot of experimental and calculated ring current increments for (*R*)-**3**. i and ii calculated by semiclassical and iii by quantum-mechanical methods.

from the data reported by Bovey and Johnson^{5a,b} (i and ii) and Haigh and Mallion (iii).^{6a,b} Straight lines were fitted to the plots, and in all cases regression coefficients were essentially unmodified by the inclusion of data for [10]paracyclophane^{5e} (without correction for local anisotropic contributions^{5d}). The plots indicate that ring current increments calculated in accordance with the quantum-mechanical model⁶ (slope = 0.392) are the less accurate, while those obtained by the semiclassical approach closely agree with the experimental values ((i) slope = 1.063 and (ii) 1.168 for ring-current intensity, coefficient = 1 and 1.09 in benzene ring current intensity units respectively).^{5c}

(15) See ref 12, p 86.

(16) (a) Binsch, G. *J. Am. Chem. Soc.* **1969**, *91*, 1304-1309. (b) Kleier, D. A.; Binsch, G. *J. Magn. Reson.* **1970**, *3*, 146-160.

(17) Friebolin, H. *Basic one- and two-dimensional NMR spectroscopy*; VCH: Weinheim, 1991.

(18) Michinori, Oki. *Application of dynamic NMR spectroscopy to organic chemistry*; VCH: Weinheim, 1985.

The calculated and experimental ring current increments for the SCs of the other esters studied are also listed in Table 2. In (*S*)-esters, whose SCs are in the less stable ap conformation, the calculated ring current increments are similar in magnitude to those of (*R*)-esters; the degree to which these shifts are reflected in their spectra is thus dependent on the relative populations of the SC and NSC. Ring current increments are appreciable in the spectra of all (*S*) esters (e.g., Me(9') in (*S*)-**2** resonates at 0.631 ppm, as against 0.768 ppm in (-)-menthol), suggesting that the population of the SCs in these isomers is significant.

For both (*R*)- and (*S*)-esters, experimental ring current increments closely agree with the calculated values, particularly those obtained by semiclassical methods, and so corroborate the molecular geometries proposed for AMAAs in this work.

Ground State Energy of AMAA Esters and Stereoselectivity

The above results indicate that esters of AMAA have the C_α-OMe and C=O groups *sinperiplanar* (*sp*) in the major conformers and antiperiplanar (*ap*) in the minor conformers. Rotation around the C_α-OMe bond can occur in each of these conformers, the lowest energy rotamer being the one with the methoxy methyl *gauche* to the C=O and *anti* to the aryl ring. In esters with nonsymmetrically substituted aryl rings (**2** and **3**), rotation around the C_α-Ar bond leads to two stable conformations, the lowest energy one having H(8) of the naphthyl ring *anti* to C_α-H.

The energy difference between the *sp* and *ap* conformations evaluated from the DNMR experiments and by comparison of the calculated and experimental ring current increments shows that the *ap* conformation has higher energy than the *sp* conformation in all compounds and that the *ap/sp* energy difference for the (*S*) isomers is, on average, 0.5 kcal/mol greater than that for the (*R*) isomers (cf. 0.9 against 0.6 kcal/mol calculated by AM1 for (*S*)-**1** and (*R*)-**1**, respectively). This *ap/sp* energy difference may be due to destabilizing interactions between the AMAA and alcohol moieties of the esters; for example, the *sp* conformation of (*R*)-**3** (SC) has the H(7') of menthol only 2.84 Å from the ring plane. Such destabilization of the *sp* conformation of (*R*)-esters and the *ap* conformation of (*S*)-esters may account for the occasional failure of the "Mosher method" for chiral recognition.^{3a-d}

The population of the *sp* conformation of both (*R*)- and (*S*)-esters increases when the phenyl ring is replaced by 1-naphthyl or by 9-anthryl (i.e., from **1** to **3** and from **3** to **4**), possibly because of enhancement of stabilizing interactions between the aryl and the C=O groups. The *sp* conformation of esters of AMAAs may therefore be stabilized by the introduction of bulkier aryl rings. Such changes lead to improved reagents for the NMR recognition of chirality of alcohols.⁷ In addition, our DNMR studies indicate that the conformational equilibria of esters of AMAAs can be significantly altered by changes in the probe temperature, and this might also be of use in that NMR application.

Besides that, our results show that in (*R*)- and (*S*)-AMAA esters the α-aryl ring must lie in the more stable conformer almost "perpendicular" to the C=O bond in order to minimize electrostatic and steric interactions. This geometry is coincident with that proposed for the

transition state of Diels–Alder reactions employing α-methoxy-α-phenylacetic acid (MPA), as a chiral auxiliary,^{1b,d} and is also in good agreement with *ab initio* calculations.^{1c} Moreover, AM1 calculations and DNMR spectroscopy indicate that at 298 K, ca. 70% of the (*R*)-**1** molecules have this ground state conformation and ca. 82% at 153 K (similar results are obtained for (*S*)-**1**) in accordance with the increased diastereofacial stereoselectivity (from 82:18 to 94:6) observed for the Diels–Alder reaction between (*S*)-α-methoxy-α-(phenylacetoxy)butadiene and acrolein in the temperature range 253–195 K.^{1b}

Experimental Section

Computational Methods. Molecular mechanics and molecular dynamics (employing the CV force field¹⁹) and AM1 molecular orbital calculations were performed by the Insight II package on a Silicon Graphics Iris computer. Initial molecular geometries of esters **1–6** originated from the Builder Module of Insight II; 3D coordinates were then generated from the bond lengths, bond angles, and dihedral angles by the DG-II package.²⁰ The conformational space of each compound was scanned by MM optimization of the sterically allowed conformations around key single bonds and by means of high-temperature molecular dynamics simulations. The latter were performed at 300, 600, and 900 K, with time steps of 1.0 fs and for a total interval of 10–30 ps; structures were sampled every 0.2 ps. Analysis of conformational transitions, identification of the low-energy conformers, and calculation of the energy barriers between these conformers were all carried out by MM with an additional harmonic term of the form $k(1 + \cos(n\theta - \theta_0))$ included in the force field. The energies of conformations were minimized in Cartesian coordinate space by the block-diagonal Newton–Raphson method; minima corresponded to root mean square (rms) energy gradients < 0.001 kcal/mol Å. The ground state energies of the geometries were then calculated by AM1^{21a} using the MOPAC 6.0 program. For all compounds, full geometry optimization used the Broyden–Fletcher–Goldfarb–Shanno (BFGS) method and the PRECISE option.^{21a,b}

NMR Spectroscopy. ¹H and ¹³C NMR spectra of samples in 4:1 CS₂/CD₂Cl₂ (4 mg in 0.5 mL) were recorded on Bruker AMX 500, AMX 300, and WM 250 NMR spectrometers. Chemical shifts (ppm) are internally referenced to the TMS signal (0 ppm) in all cases.

1D ¹H NMR spectra: size 32 K, pulse length 2.8 μs (30°), 16 acquisitions.

1D ¹³C NMR spectra: size 64 K, pulse length 3.5 μs (30°), 1024 acquisitions.

2D COSY spectra: sequence: D1-90-t1-90-t2; relaxation delay D1 = 0.5 s; 90° pulse 8.5 μs.

2D NOESY spectrum: sequence D1-90-t1-90-τ_{mix}-90-t2; relaxation delay D1 = 0.5 s; mixing time (τ_{mix}) 0.5 s; 90° pulse 8.5 μs; TPPI-mode, NS = 64.

Proton-detected heteronuclear multiple quantum correlation (HMQC) experiments. Sequence: D1-BIRD-D4-90(¹H)-D2-90(¹³C)-t₁/2-180(¹H)-t₁/2-90(¹³C)-D2-t₂ (GARP(¹³C)), relaxation delay D1 = 2s; D2 = 3.45 ms; D4 = 0.3 s; 90° pulse (¹H) 8.5 μs; 90° pulse (¹³C) 10.5 μs.

For DNMR spectroscopy, the probe temperature was controlled by a standard unit calibrated using a methanol reference; samples were allowed to equilibrate for 15 min at each temperature before recording spectra.

Line shape analysis (temperature intervals are quoted in the text) of signals broadened by chemical exchange was carried out by the DNMR5 program¹⁶ (Fortran 77) on an Aspect 3000 computer. Rate constants evaluated from these

(19) Roberts, V. A.; Osguthorpe, D. I.; Wolff, J.; Genest, M.; Hagler, A. T. *Proteins: Struct., Funct. Genet.* **1988**, *4*, 31.

(20) Cioslowski, J.; Kertesz, M. *QCPE Bull.* **1987**, *7*, 159.

(21) (a) Dewar, M. J. S.; Zoebisch, E. G.; Healy, E. F.; Stewart, J. J. P. *J. Am. Chem. Soc.* **1985**, *107*, 3902–3909. (b) Havel, T. F. *Prog. Mol. Biol. Biophys.* **1991**, *56*, 43.

data were used to calculate activation parameters by means of the Eyring equation.¹⁷

General. The esters 1–6 were prepared by treatment of alcohol with the corresponding acid in the presence of DCC and DMAP (catalytic)^{2b} followed by purification by HPLC (7.8 mm × 30 mm, μ -Porasil, hexane–ethyl acetate, 96–4, 1.2 mL/min).

Racemic hydroxynaphthylacetic acids were prepared from corresponding arylaldehydes through the cyanohydrin²² (method 1) or trimethylsilylcyanohydrin²³ (method 2) method, followed by acid hydrolysis.

Racemic (hydroxyanthryl)acetic acid was obtained by reduction of ethyl (9-anthryl)glyoxylate with NaBH₄.

In all cases the *O*-methylarylacetic acids were obtained by treatment of methyl esters with methyl iodide followed by basic hydrolysis.

Optically pure arylmethoxyacetic acids were isolated from the racemic mixture by HPLC on a chiral column (6 mm × 30 mm, MW 31, modified cellulose). In each pair of enantiomers the *R* presents, on this column, a shorter retention time than its enantiomer. Absolute configuration of all arylmethoxyacetic acids was determined by CD. All the *R* acids present negative optical rotation, negative first Cotton effect and positive second one, all the *S* acids have the opposite values.

(±)- α -Hydroxy- α -(1-naphthyl)acetic Acid (7). Compound 7 (1.79 g, 63% yield, method 1; 2.68 g, 96.6%, method 2) was obtained from 1 mL of 1-naphthaldehyde as an oil: ¹H NMR (250.13 MHz, CD₃OD) δ (ppm) 5.8 (s, 1H), 7.4–8.3 (m, 7H); ¹³C NMR (62.83 MHz, CD₃OD) δ (ppm) 72.6, 125.5, 126.4, 126.8, 127.1, 127.3, 129.7, 130.1, 132.6, 135.6, 136.7, 176.8; IR (NaCl) 3435, 3049, 3015, 2953, 2342, 1939, 1738, 1650, 1597, 1511, 1437, 1395, 1216, 1165, 1094, 1064, 972, 922 cm⁻¹; UV λ_{\max} 220 nm (MeOH); MS (EI) *m/z* 202 (M⁺); HRMS(EI) C₁₂H₁₀O₃ obsd 202.0645, calcd 202.062 89 Δm 1.15 mu.

Anal. Calcd for C₁₂H₁₀O₃: C, 71.28; H, 4.95; O, 23.76. Found: C, 71.30; H, 4.94; O, 23.75.

(±)- α -Hydroxy- α -(2-naphthyl)acetic Acid (8). Two g of 2-naphthaldehyde was treated as above affording 2 g of 8 (77% yield, method 1) and 1.8 g of 8 (74% yield, method 2): mp 155 °C (C₆H₆); ¹H NMR (250.13 MHz, CD₃OD) δ (ppm) 5.39 (s, 1H), 7.35–7.99 (m, 7H); ¹³C NMR (62.83 MHz, CD₃OD) δ (ppm) 74.4, 125.7, 127.1, 127.3, 137.4, 128.8, 129.1, 129.28, 134.8, 138.3, 176.3; IR (NaCl) 3569, 3373, 3020, 2954, 2925, 2850, 1715, 1598, 1446, 1368, 1221, 1167, 1071, 948, 857, 750, 704 cm⁻¹; UV λ_{\max} 228 nm (MeOH); MS (EI) *m/z* 202 (M⁺); HRMS(EI) C₁₂H₁₀O₃ obsd 202.0635, calcd 202.062 99 Δm 0.51 mu.

Anal. Calcd for C₁₂H₁₀O₃: C, 71.28; H, 4.95; O, 23.76. Found: C, 71.26; H, 4.94; O, 23.79.

(±)-Methyl α -Hydroxy- α -(1-naphthyl)acetate (9). A 1.17 g portion of 9 was prepared from 1.5 g of 7 (73% yield): mp 80 °C (Cl₂CH₂); ¹H NMR (250.13 MHz, CDCl₃) δ (ppm) 3.69 (s, 3H), 5.82 (s, 1H), 7.42–8.21 (m, 7H); ¹³C NMR (62.83 MHz, CDCl₃) δ (ppm) 52.7, 71.2, 123.6, 125.1, 125.7, 126.5, 128.7, 129.3, 130.9, 133.9, 134.0, 174.5; IR (NaCl) 3500, 3010, 2950, 2850, 1750, 1600, 1510, 1425, 1250, 1100, 950, 750 cm⁻¹; UV λ_{\max} 220 nm (MeOH); MS (EI) *m/z* 216 (M⁺); HRMS(EI) C₁₃H₁₂O₃ obsd 216.0793, calcd 216.078 64 Δm 7.6 mu.

(±)-Methyl α -Hydroxy- α -(2-naphthyl)acetate (10). A 1.8 g (8.9 mmol) portion of 8 was treated as above affording 1.49 g of 10 (78% yield): mp 85 °C (Cl₂CH₂); ¹H NMR (250.13 MHz, CDCl₃) δ (ppm) 3.74 (s, 3H), 5.39 (s, 1H), 7.48–7.93 (m, 7H); ¹³C NMR (62.83 MHz, CDCl₃) δ (ppm) 52.7, 72.9, 124.0, 125.8, 126.2, 127.5, 128.0, 128.3, 133.1, 133.2, 135.6, 173.2; IR (NaCl) 3500, 3050, 3010, 2950, 2850, 1750, 1600, 1500, 1450, 1350, 1275, 1250, 1150, 1110, 750 cm⁻¹; UV λ_{\max} 220 nm (MeOH); MS (EI) *m/z* 216 (M⁺); HRMS(EI) C₁₃H₁₂O₃ obsd 216.0792, calcd 216.078 64 Δm 1.56 mu.

Ethyl (9-Anthryl)glyoxylate (11). Two g of anthracene (11 mmol) was treated with 1.25 mL of ethyl oxalyl chloride (12 mmol) affording 3.051 g (97% yield) of 11 after further purification by flash chromatography: mp 85 °C (Cl₃CH); ¹H

NMR (300 MHz, CDCl₃) δ (ppm) 1.30 (t, *J* = 7 Hz, 3H), 4.36 (q, *J* = 7 Hz, 2H), 7.44–8.53 (m, 9H); ¹³C NMR (74, 77 MHz, CDCl₃) δ (ppm) 14.2, 63.2, 129.5, 124.2, 125.9, 126.6, 128.0, 129.1, 129.3, 130.3, 131.5, 163.3; IR (NaCl) 3050, 2950, 2300, 1725, 1600, 1450, 1400, 1300, 1250, 1100 cm⁻¹; UV λ_{\max} 254 nm (Cl₃CH); MS (EI) *m/z* 278 (M⁺); HRMS(EI) C₁₈H₁₄O₃ obsd 278.0941, calcd 278.094 29 Δm 0.19 mu.

(±)-Ethyl α -Hydroxy- α -(9-anthryl)acetate (12). A 2.8 g portion of 10 (10 mmol) was reduced with NaBH₄ to obtain 2.819 g (99% yield) of compound 12: mp 110 °C (Cl₂CH₂); ¹H NMR (300 MHz, CDCl₃) δ (ppm) 0.98 (t, *J* = 7 Hz, 3H), 4.13 (q, *J* = 7 Hz, 2H), 6.56 (s, 1H), 7.40–8.41 (m, 9H); ¹³C NMR (74.77 MHz, CDCl₃) δ (ppm) 12.6, 61, 66.9, 122.6, 123.7, 125.3, 127.3, 128.0, 129.1, 130.3, 173.9; IR (NaCl) 3500, 3150, 3050, 3000, 2950, 2350, 1725, 1450, 1410, 1300, 1100 cm⁻¹; UV λ_{\max} 254 nm (Cl₃CH); MS (EI) *m/z* 280 (M⁺); HRMS(EI) C₁₈H₁₆O₃ obsd 280.109 60, calcd 280.109 94 Δm 0.34 mu.

(±)-Methyl α -Methoxy- α -(1-naphthyl)acetate (13). Compound 9 (1.1 g, 5 mmol) was treated with silver oxide and MeI affording 0.85 g of compound 13 as an oil (74% yield): ¹H NMR (250.13 MHz, CDCl₃) δ (ppm) 3.46 (s, 3H), 3.67 (s, 3H), 5.41 (s, 1H), 7.47–8.33 (m, 7H); ¹³C NMR (62.83 MHz, CDCl₃) δ (ppm) 52.1, 57.3, 81.1, 123.9, 125.1, 125.8, 126.5, 126.7, 128.7, 129.4, 132.1, 132.1, 133.9, 171.2; IR (NaCl) 3000, 2950, 2850, 1700, 1600, 1500, 1450, 1350, 1200, 1100, 1000, 900, 750 cm⁻¹; UV λ_{\max} 262 nm (MeOH); MS (EI) *m/z* 230 (M⁺); HRMS(EI) C₁₄H₁₄O₃ obsd 230.0962, calcd 230.094 29 Δm 1.91 mu.

(±)-Methyl α -Methoxy- α -(2-naphthyl)acetate (14). A 1.25 g portion of 14 was obtained from 1.4 g of 10 treated as above (84% yield): ¹H NMR (250.13 MHz, CDCl₃) δ (ppm) 3.46 (s, 3H), 3.72 (s, 3H), 4.96 (s, 1H), 7.47–7.94 (m, 7H); ¹³C NMR (62.83 MHz, CDCl₃) δ (ppm) 52.1, 57.2, 82.6, 124.3, 126.3, 126.3, 126.7, 127.6, 128.1, 128.5, 133.1, 133.4, 133.5, 171.1; IR (NaCl) 3050, 3000, 2950, 2900, 2300, 1700, 1600, 1500, 1450, 1250, 1000, 700 cm⁻¹; UV λ_{\max} 220 nm (MeOH); MS (EI) *m/z* 230 (M⁺); HRMS(EI) C₁₄H₁₄O₃ obsd 230.0947, calcd 230.0950 Δm 0.3 mu.

(±)-Ethyl α -Methoxy- α -(9-anthryl)acetate (15). In the same way, 1.7 g of 15 was obtained from 2.2 g of 12 (57.82% yield): mp 75–80 °C (Cl₂CH₂); ¹H NMR (300 MHz, CDCl₃) δ (ppm) 0.95 (t, *J* = 7 Hz, 3H), 3.39 (s, 3H), 4.06 (q, *J* = 7 Hz, 2H), 6.28 (s, 1H), 7.39–8.6 (m, 9H); ¹³C NMR (74.77 MHz, CDCl₃) δ (ppm) 13.7, 51.4, 61.1, 76.9, 124.4, 124.7, 126.3, 127.2, 128.9, 129.1, 130.3, 131.2, 171.2; IR (NaCl) 3050, 3025, 2950, 2900, 2800, 1750, 1650, 1525, 1450, 1325, 1200, 1100, 1025, 700 cm⁻¹; UV λ_{\max} 262 nm (Cl₃CH); MS (EI) *m/z* 294 (M⁺); HRMS(EI) C₁₉H₁₈O₃ obsd 294.125 70, calcd 294.125 59 Δm 0.11 mu.

(±)- α -Methoxy- α -(1-naphthyl)acetic Acid (16). A 0.59 g portion of 16 was obtained from 0.85 g of 13 by alkali hydrolysis (75% yield): mp 155 °C (Cl₃CH); ¹H NMR (250.13 MHz, CDCl₃) δ (ppm) 3.46 (s, 3H), 5.41 (s, 1H), 7.43–8.26 (m, 7H); ¹³C NMR (62.83 MHz, CDCl₃) δ (ppm) 57.3, 80.7, 123.9, 125.2, 126.1, 126.7, 127.1, 128.8, 129.8, 131.1, 131.4, 134.1, 175.1; IR (NaCl) 3500, 3450–3150, 3050, 2950, 1775, 1725, 1600, 1500, 1100, 700 cm⁻¹; UV λ_{\max} 216 nm (MeOH); MS (EI) *m/z* 216 (M⁺); HRMS(EI) C₁₃H₁₂O₃ obsd 216.0798, calcd 216.078 64 Δm 1.16 mu.

Anal. Calcd for C₁₃H₁₂O₃: C, 72.22; H, 5.55; O, 22.22. Found: C, 72.25; H, 5.54; O, 22.20.

(-)-(*R*)- α -Methoxy- α -(1-naphthyl)acetic acid ((*R*)-16): HPLC *t_R* = 31.16 min; [α] = -130.66 (*c* = 0.003, EtOH); CD (*c* = 5.5 × 10⁻⁵ M, EtOH); λ_{\max} /nm ($\Delta \epsilon$ /cm² mol⁻¹) 230 (-18.34), 216 (10.35).

(+)-(*S*)- α -Methoxy- α -(1-naphthyl)acetic acid ((*S*)-16): HPLC *t_R* = 34.02 min; [α] = +134.5 (*c* = 0.004, EtOH); CD (*c* = 5.3 × 10⁻⁵ M, EtOH); λ_{\max} /nm ($\Delta \epsilon$ /cm² mol⁻¹) 230 (18.45), 216 (-12.9).

(±)- α -Methoxy- α -(2-naphthyl)acetic Acid (17). A 1.25 g portion of 14 treated as before yield 0.72 g of 17 (62%): mp 98 °C (Cl₃CH); ¹H NMR (250.13 MHz, CDCl₃) δ (ppm) 3.38 (s, 3H), 4.91 (s, 1H), 7.46–7.89 (m, 7H); ¹³C NMR (62.83 MHz, CDCl₃) δ (ppm) 82.4, 124.4, 126.4, 126.5, 127.1, 127.7, 128.2, 128.7, 133.0, 133.2, 133.6, 175.3; IR (NaCl) 3500, 3200, 3010, 2975, 2900, 1700, 1600, 1450, 1250, 1100, 750 cm⁻¹; UV λ_{\max}

(22) Pohl, L. R.; Trager, W. F. *J. Med. Chem.* **1973**, *16*, 475–479.

(23) Gassman, P. G.; Talley, J. L. *Tetrahedron Lett.* **1978**, *40*, 3773–3776.

216 nm (MeOH); MS (EI) m/z 216 (M^+); HRMS(EI) $C_{13}H_{12}O_3$ obsd 216.0799, calcd 216.078 64 Δm 1.16 mu.

Anal. Calcd for $C_{13}H_{12}O_3$: C, 72.22; H, 5.55; O, 22.22. Found: C, 72.18; H, 5.51; O, 22.19.

(-)-(*R*)- α -Methoxy- α -(2-naphthyl)acetic acid (*R*)-17: HPLC t_R = 26.64 min; $[\alpha] = -120.8$ ($c = 0.005$, EtOH); CD ($c = 4.6 \times 10^{-5}$ M, EtOH); λ_{max}/nm ($\Delta\epsilon/cm^2 mol^{-1}$) 230 (-11.56), 215 (6.30).

(+)-(*S*)- α -Methoxy- α -(2-naphthyl)acetic acid (*S*)-17: HPLC t_R = 29.01 min; $[\alpha] = +120$ ($c = 0.0015$, EtOH); CD ($c = 2.7 \times 10^{-5}$ M, EtOH); λ_{max}/nm ($\Delta\epsilon/cm^2 mol^{-1}$) 230 (-6.86), 215 (-6.7).

(\pm)- α -Methoxy- α -(9-anthryl)acetic Acid (18). A 1.7 g portion of 15 treated as above afforded 1.5 g of 18 (97.5% yield): mp 190 °C (Cl_3CH); 1H NMR (250.13 MHz, $CDCl_3$) δ (ppm) 3.38 (s, 3 H), 6.31 (s, 1 H), 7.44–7.56 (m, 4 H), 8.01–8.05 (m, 2 H), 8.43–8.50 (m, 3 H); ^{13}C NMR (62.83 MHz, $CDCl_3$) δ (ppm) 57.3, 76.5, 124.0, 125.1, 126.1, 126.8, 129.3, 129.8, 130.8, 131.5, 174.5; IR (NaCl) 3650 3500–3250, 3025, 2900, 2350, 1680, 1425, 1200, 1100, 900 cm^{-1} ; UV λ_{max} 300 nm (CH_3OH); MS (EI) m/z 266 (M^+); HRMS(EI) $C_{17}H_{14}O_3$ obsd 266.094 40, calcd 266.094 29 Δm 0.11 mu.

Anal. Calcd for $C_{17}H_{14}O_3$: C, 76.69; H, 5.26; O, 18.04. Found: C, 76.65; H, 5.22; O, 18.02.

(-)-(*R*)- α -Methoxy- α -(9-anthryl)acetic acid (*R*)-18: HPLC t_R = 7.77 min; $[\alpha] = -131.25$ ($c = 0.0016$, EtOH); CD ($c = 6 \times 10^{-5}$ M, EtOH); λ_{max}/nm ($\Delta\epsilon/cm^2 mol^{-1}$) 260 (-23.71), 244 (12.32).

(+)-(*S*)- α -Methoxy- α -(9-anthryl)acetic acid (*S*)-18: HPLC t_R = 9.62 min; $[\alpha] = +133.75$ ($c = 0.0016$, EtOH); CD ($c = 6 \times 10^{-5}$ M, EtOH); λ_{max}/nm ($\Delta\epsilon/cm^2 mol^{-1}$) 260 (23.08), 245 (-11.97).

(-)-Menthyl (-)-(*R*)- α -Methylmandelate (*R*)-1. A 54 mg portion of (*R*)-1 was obtained from 33 mg of (*R*)-MPA and 37 mg of (-)-menthol (90% yield): HPLC t_R = 19.46 min; $[\alpha] = -53.94$ ($c = 0.000$ 76, EtOH); 1H NMR (250.13 MHz, $CDCl_3$) δ (ppm) 0.43 (d, $J = 6.9$ Hz, 3H), 0.63 (d, $J = 6.9$ Hz, 3 H), 0.89 (d, $J = 6.3$ Hz, 3 H), 0.91–2.05 (m, 9 H), 3.25 (s, 3 H), 4.6 (ddd, $J = 6.5$ Hz, $J' = J'' = 10.8$ Hz, 1 H), 4.71 (s, 3 H), 7.31–7.41 (m, 5 H); ^{13}C NMR (62.83 MHz, $CS_2 + C_2D_2Cl_2$ 4:1) δ (ppm) 15.6, 20.5, 22.1, 23.3, 25.4, 31.5, 34.4, 40.8, 47.1, 56.7, 74.4, 82.7, 127.1, 128.3, 136.8, 169.2; IR (NaCl) 2960, 2921, 2870, 1740, 1455, 1367, 1267, 1186, 1110, 997, 913, 734, 678 cm^{-1} ; 1H NMR [500 MHz, $CS_2 + CD_2Cl_2$ 4:1, 298 K, δ (ppm)] 4.44 ($H1'$), 1.23 ($H2'$), 1.58 ($H3'$ eq), 0.95 ($H3'$ ax), 1.62 ($H4'$ eq), 0.8 ($H4'$ ax), 1.4 ($H5'$), 1.9 ($H6'$), 1.25 ($H7'$), 0.65 ($H8'$), 0.41 ($H9'$), 0.89 ($H10'$); 1H NMR [500 MHz, $CS_2 + CD_2Cl_2$ 4:1, 153 K, δ (ppm)] 0.80 ($H7'$), 0.89 ($H10'$).

(-)-Menthyl (+)-(*S*)- α -Methylmandelate (*S*)-1. A 43 mg portion of (*S*)-1 was obtained from 25 mg of (*S*)-MPA and 28 mg of (-)-menthol (93% yield): HPLC t_R = 18.02 min; $[\alpha] = -7.52$ ($c = 0.000$ 93, EtOH); 1H NMR (250.13 MHz, $CDCl_3$) δ (ppm) 0.69 (d, $J = 6.66$ Hz, 3 H), 0.84 (d, $J = 6.3$ Hz, 6 H), 0.91–2.05 (m, 9 H), 3.41 (s, 3 H), 4.71 (ddd, $J = 6.5$, $J' = J'' = 10.8$ Hz, 1 H), 4.74 (s, 1H), 7.32–7.42 (m, 5H); ^{13}C NMR (62.83 MHz, $CS_2 + Cl_2CD_2$ 4:1) δ (ppm) 16.1, 20.6, 22.1, 23.6, 24.9, 25.9, 26.2, 31.4, 53.6, 56.8, 74.3, 82.6, 126.8, 128.2, 136.6, 169.2; IR (NaCl) 2960, 2929, 2867, 1737, 1455, 1358, 1263, 1186, 1109, 996, 842, 735, 699 cm^{-1} ; 1H NMR [500 MHz, $CS_2 + CD_2Cl_2$ 4:1, 298 K, δ (ppm)] 4.56 ($H1'$), 1.3 ($H2'$), 1.60 ($H3'$ eq), 1.0 ($H3'$ ax), 1.6 ($H4'$ eq), 0.80 ($H4'$ ax), 1.36 ($H5'$), 1.70 ($H6'$ eq), 0.74 ($H6'$ ax), 1.70 ($H7'$), 0.84 ($H8'$), 0.64 ($H9'$), 0.82 ($H10'$); 1H NMR [500 MHz, $CS_2 + CD_2Cl_2$ 4:1, 163 K, δ (ppm)] 1.60 ($H6'$ eq), 1.87 ($H7'$), 0.89 ($H8'$), 0.68 ($H9'$), 0.79 ($H10'$).

(-)-Menthyl (-)-(*R*)- α -O-Methyl- α -(2-naphthyl)acetate (*R*)-2. A 63 mg portion of (*R*)-2 was obtained from 40 mg of (*R*)-17 and 28 mg of (-)-menthol (97% yield): HPLC t_R = 30.78 min; $[\alpha] = -47.33$ ($c = 0.006$, EtOH); 1H NMR (250.13 MHz, $CDCl_3$) δ (ppm) 0.34 (d, $J = 6.9$ Hz, 3 H), 0.47 (d, $J = 6.9$ Hz, 3 H), 0.80 (d, $J = 6.5$ Hz, 3 H), 0.79–1.92 (m, 9 Hz), 3.45 (s, 3 H), 4.66 (ddd, $J = 4.3$ Hz, $J' = J'' = 10.6$ Hz, 1 H), 4.89 (s, 1 H), 7.4–7.92 (m, 7 H); ^{13}C NMR (62.83 MHz, $CS_2 + Cl_2CD_2$ 4:1) δ (ppm): 15.5, 20.4, 22.2, 23.3, 25.5, 31.5, 34.5, 40.8, 47.1, 56.8, 74.5, 82.8, 124.6, 126.2, 126.6, 127.6, 128.1, 133.0, 133.2, 134.2, 169.1; IR (NaCl) 3057, 2951, 1918, 2855, 2118, 1742, 1451, 1368, 1338, 1191, 1108, 1010, 812 cm^{-1} ; UV λ_{max} 224

nm (CH_3OH); MS (EI) m/z 354 (M^+); HRMS(EI) $C_{23}H_{30}O_3$ obsd 354.2165, calcd 354.219 48 Δm 1.98 mu. 1H NMR [500 MHz, $CS_2 + CD_2Cl_2$ 4:1, 298 K, δ (ppm)] 4.50 ($H1'$), 1.2 ($H7'$), 0.53 ($H8'$), 0.34 ($H9'$), 0.87 ($H10'$); 1H NMR [500 MHz, $CS_2 + CD_2Cl_2$ 4:1, 153 K, δ (ppm)] 4.44 ($H1'$), 0.52 ($H7'$), 0.44 ($H8'$), 0.12 ($H9'$), 0.89 ($H10'$).

Anal. Calcd for $C_{23}H_{30}O_3$: C, 77.96; H, 8.57; O, 13.55. Found: C, 77.95; H, 8.50; O, 13.56.

(-)-Menthyl (+)-(*S*)- α -O-Methyl- α -(2-naphthyl)acetate (*S*)-2. A 52 mg portion of (*S*)-2 was obtained from 38 mg of (*S*)-17 and 27 mg of (-)-menthol (84% yield): HPLC t_R = 29.32; $[\alpha] = +1$ ($c = 0.004$, EtOH); 1H NMR (250.13 MHz, $CDCl_3$) δ (ppm) 0.69 (d, $J = 6.9$ Hz, 3 H), 0.84 (d, $J = 7.1$ Hz, 3 H), 0.88 (d, $J = 6.5$ Hz, 3H), 0.97–1.92 (m, 9 H), 3.45 (s, 3 H), (ddd, $J = 4.3$ Hz, $J' = J'' = 10.6$ Hz, 1 H), 4.91 (s, 1 H), 7.42–7.92 (m, 7 H); ^{13}C NMR (62.83 MHz, $CS_2 + Cl_2CD_2$ 4:1) δ (ppm) 16.1, 20.6, 22.1, 23.6, 26.1, 31.5, 34.1, 40.4, 47.1, 55.4, 74.4, 82.7, 124.5, 126.2, 126.3, 127.7, 128.1, 133.1, 133.2, 134.1, 169.1; IR (NaCl) 3055, 2923, 2852, 2116, 1741, 1451, 1189, 1107, 1010 cm^{-1} ; UV λ_{max} 225 nm (CH_3OH); MS (EI) m/z 354 (M^+); 1H NMR [500 MHz, $CS_2 + CD_2Cl_2$ 4:1, 298 K, δ (ppm)] 4.59 ($H1'$), 1.75 ($H7'$), 0.80 ($H8'$), 0.63 ($H9'$), 0.81 ($H10'$); 1H NMR [500 MHz, $CS_2 + CD_2Cl_2$ 4:1, 153 K, δ (ppm)] 4.60 ($H1'$), 1.80 ($H7'$), 0.89 ($H8'$), 0.71 ($H9'$), 0.71 ($H10'$).

Anal. Calcd for $C_{23}H_{30}O_3$: C, 77.96; H, 8.57; O, 13.55. Found: C, 77.99; H, 8.43; O, 13.53.

(-)-Menthyl (-)-(*R*)- α -O-Methyl- α -(1-naphthyl)acetate (*R*)-3. A 37 mg portion of (*R*)-3 was obtained from 25 mg of (*R*)-16 and 18 mg of (-)-menthol (92% yield): HPLC t_R = 19.16 min; $[\alpha] = -87.14$ ($c = 0.0021$, EtOH); 1H NMR (250.13 MHz, $CDCl_3$) δ (ppm) 0.01 (d, $J = 6.8$ Hz, 3 H), 0.31 (d, $J = 6.9$ Hz), 4.58 (ddd, $J = 4.2$ Hz, $J' = J'' = 10.8$ Hz, 1 H), 5.31 (s, 1 H), 7.26–8.33 (m, 7 H); ^{13}C NMR (62.83 MHz, $CS_2 + Cl_2CD_2$ 4:1) δ (ppm) 15.2, 20.3, 22.1, 23.2, 25.1, 31.5, 34.4, 40.9, 47.1, 57.1, 74.7, 81.6, 124.3, 124.6, 125.1, 125.8, 126.2, 126.8, 128.5, 129.1, 169.4; IR (NaCl) 3039, 2978, 2928, 2852, 1740, 1593, 1513, 1457, 1375, 1261, 1192, 1107, 986 cm^{-1} ; UV λ_{max} 224 nm (EtOH); MS (EI) m/z 354 (M^+); HRMS(EI) $C_{23}H_{30}O_3$ obsd 354.2173, calcd 354.219 48 Δm 2.18 mu; 1H NMR [500 MHz, $CS_2 + CD_2Cl_2$ 4:1, 298 K, δ (ppm)] 4.4 ($H1'$), 1.02 ($H2'$), 1.45 ($H3'$ eq), 0.8 ($H3'$ ax), 1.59 ($H4'$ eq), 0.75 ($H4'$ ax), 1.37 ($H5'$), 1.90 ($H6'$ eq), 0.85 ($H6'$ ax), 0.72 ($H7'$), 0.32 ($H8'$), 0.09 ($H9'$), 0.83 ($H10'$); 1H NMR [500 MHz, $CS_2 + CD_2Cl_2$ 4:1, 153 K, major component (A), δ (ppm)] 4.25 ($H1'$), 0.85 ($H2'$), 0.75 ($H3'$ ax), 1.60 ($H4'$ eq), 1.40 ($H5'$), -0.16 ($H7'$), 0.15 ($H8'$), -0.47 ($H9'$), 0.85 ($H10'$); second component (B) 0.95 ($H7'$), 0.41 ($H8'$), 0.33 ($H9'$); minor component (C) 0.90 ($H8'$), 0.76 ($H9'$).

Anal. Calcd for $C_{23}H_{30}O_3$: C, 77.96; H, 8.57; O, 13.55. Found: C, 77.93; H, 8.50; O, 13.52.

(-)-Menthyl (+)-(*S*)- α -O-Methyl- α -(1-naphthyl)acetate (*S*)-3. A 47 mg portion of (*S*)-3 was obtained from 30 mg of (*S*)-16 and 21 mg of (-)-menthol (96% yield): HPLC t_R = 17.10 min; $[\alpha] = -1.85$ ($c = 0.001$, EtOH); 1H NMR (250.13 MHz, $CDCl_3$) δ (ppm) 0.66 (d, $J = 6.9$ Hz, 3 H), 0.76 (d, $J = 6.7$ Hz, 3 H), 0.83 (d, $J = 7$ Hz, 3 H), 0.92–2.01 (m, 9 H), 3.46 (s, 3 H), 4.73 (ddd, $J = 4.2$ Hz, $J' = J'' = 10.8$ Hz), 5.38 (s, 1 H), 7.43–8.26 (m, 7 H); ^{13}C NMR (62.83 MHz, $CS_2 + Cl_2CD_2$ 4:1) δ (ppm) 16.1, 20.6, 22.1, 23.6, 26.3, 31.4, 34.4, 40.3, 47.1, 57.1, 74.7, 81.2, 125.2, 125.8, 126.2, 129.1, 131.7, 132.7, 133.8, 169.4; IR (NaCl) 3055, 2981, 2824, 1741, 1457, 1368, 1294, 1253, 1154, 1111, 993, 846 cm^{-1} ; UV λ_{max} 224 nm (CH_3OH); MS (EI) m/z 354 (M^+); 1H NMR [500 MHz, $CS_2 + CD_2Cl_2$ 4:1, 298 K, δ (ppm)] 4.38 ($H1'$), 1.22 ($H2'$), 1.58 ($H3'$ eq), 0.95 ($H3'$ ax), 1.58 ($H4'$ eq), 0.75 ($H4'$ ax), 1.33 ($H5'$), 1.60 ($H6'$ eq), 0.65 ($H6'$ ax), 1.65 ($H7'$), 0.78 ($H8'$), 0.59 ($H9'$), 0.78 ($H10'$); 1H NMR [500 MHz, $CS_2 + CD_2Cl_2$ 4:1, 153 K, major component (A), δ (ppm)] 1.22 ($H2'$), 1.55 ($H3'$ eq), 1.30 ($H5'$), 1.55 ($H6'$ eq), 0.62 ($H6'$ ax), 1.80 ($H7'$), 0.88 ($H8'$), 0.71 ($H9'$), 0.71 ($H10'$).

Anal. Calcd for $C_{23}H_{30}O_3$: C, 77.96; H, 8.57; O, 13.55. Found: C, 77.92; H, 8.51; O, 13.51.

(-)-Menthyl (-)-(*R*)- α -O-Methyl- α -(9-anthryl)acetate (*R*)-4. A 57 mg portion of (*R*)-4 was obtained from 43 mg of (*R*)-18 and 25 mg of (-)-menthol (87% yield): HPLC t_R = 31 min; $[\alpha] = -53.07$ ($c = 0.0026$, EtOH); 1H NMR (250.13 MHz, $CDCl_3$) δ (ppm) -0.1 (d, $J = 5.6$ Hz, 3 H), 0.43 (d, $J = 2.2$ Hz,

3 H), 0.47 (m, 1H), 0.84 (d, $J = 6.4$ Hz, 3 H), 0.89–2.01 (m, 8 H), 3.47 (s, 3 H), 4.52 (ddd, $J = 3.9$ Hz, $J' = J'' = 10.8$ Hz, 1 H), 6.35 (s, 1 H), 7.43–8.58 (m, 9 H); ^{13}C NMR (62.83 MHz, $\text{CS}_2 + \text{Cl}_2\text{CD}_2$ 4:1) δ (ppm) 15.1, 20.0, 22.2, 23.1, 24.7, 31.4, 34.3, 40.7, 46.7, 57.1, 74.5, 77.0, 124.8, 124.9, 125.9, 128.8, 128.9, 130.2, 131.2, 169.5; IR (NaCl) 3050, 2928, 2862, 1732, 1670, 1600, 1453, 1372, 1277, 1192, 1113, 1026 cm^{-1} ; UV λ_{max} 256 nm (EtOH); MS (EI) m/z 404 (M^+); ^1H NMR [500 MHz, $\text{CS}_2 + \text{CD}_2\text{Cl}_2$ 4:1, 298 K, δ (ppm)] 4.406 (H1'), 0.85 (H2'), 1.53 (H3'eq), 0.65 (H3'ax), 1.50 (H4'eq), 0.65 (H4'ax), 1.37 (H5'), 1.95 (H6'eq), 0.83 (H6'ax), 0.08 (H7'), 0.04 (H8'), -0.11 (H9'), 0.84 (H10'); ^1H NMR [500 MHz, $\text{CS}_2 + \text{CD}_2\text{Cl}_2$ 4:1, 153 K, δ (ppm)] -0.38 (H7'), -0.05 (H8'), -0.24 (H9'), 0.73 (H10').

Anal. Calcd for $\text{C}_{27}\text{H}_{32}\text{O}_3$: C, 80.19; H, 7.92; O, 11.88. Found: C, 80.17; H, 7.95; O, 11.86.

(-)-Menthyl (+)-(S)- α -O-methyl- α -(9-anthryl)acetate ((S)-4). A 49 mg portion of (S)-4 was obtained from 40 mg of (S)-18 and 23 mg of (-)-menthol (80% yield): HPLC $t_R = 29.3$ min; $[\alpha] = -4.37$ (EtOH); ^1H NMR (250.13 MHz, CDCl_3) δ (ppm) 0.37 (m, 1 H), 0.65 (d, $J = 6.5$ Hz, 3 H), 0.76 (d, $J = 7.3$ Hz, 3 H), 0.85 (d, $J = 7.1$ Hz, 3 H), 1.9–0.88 (m, 8 H), 3.38 (s, 3 H), 4.73 (ddd, $J = 3$ Hz, $J' = J'' = 10$ Hz, 1 H), 6.24 (s, 1 H), 7.44–8.56 (m, 9 H); ^{13}C NMR (62.83 MHz, $\text{CS}_2 + \text{Cl}_2\text{CD}_2$ 4:1) δ (ppm) 16.4, 20.6, 21.9, 23.6, 26.4, 31.2, 34.2, 40.0, 46.6, 57.1, 74.5, 77.1, 124.7, 124.8, 125.9, 128.5, 128.8, 130.2, 131.2, 169.4; IR (NaCl) 3045, 2930, 2865, 1735, 1670, 1596, 1455, 1306, 1194, 1110, 1009 cm^{-1} ; UV λ_{max} 256 nm ($c = 0.0029$, EtOH); MS (EI) m/z 404 (M^+); ^1H NMR [500 MHz, $\text{CS}_2 + \text{CD}_2\text{Cl}_2$ 4:1, 298 K, δ (ppm)] 4.602 (H1'), 1.12 (H2'), 1.53 (H3'eq), 0.65 (H3'ax), 1.53 (H4'eq), 0.95 (H4'ax), 1.30 (H5'), 1.45 (H6'eq), 0.31 (H6'ax), 1.80 (H7'), 0.83 (H8'), 0.73 (H9'), 0.65 (H10'); ^1H NMR [500 MHz, $\text{CS}_2 + \text{CD}_2\text{Cl}_2$ 4:1, 153 K, δ (ppm)] 1.82 (H7'), 0.75 (H8'), 0.65 (H9'), 0.58 (H10').

Anal. Calcd for $\text{C}_{27}\text{H}_{32}\text{O}_3$: C, 80.19; H, 7.92; O, 11.88. Found: C, 80.16; H, 7.94; O, 11.85.

(\pm)-Isopropyl α -O-Methyl- α -(1-naphthyl)acetate (5). A 45 mg portion of 5 was obtained from 45 mg of 16 and 12 mg

of 2-methyl-2-propanol (85% yield): ^1H NMR (300 MHz, CDCl_3) δ (ppm) 0.99 (d, $J = 6.3$ Hz, 3 H), 1.19 (d, $J = 6.3$ Hz, 3 H), 3.42 (s, 3 H), 5.04 (m, 1 H), 5.33 (s, 1 H), 7.42–8.28 (m, 7 H); ^{13}C NMR (62.83 MHz, $\text{CS}_2 + \text{Cl}_2\text{CD}_2$ 4:1) δ (ppm) 21.2, 21.5, 56.9, 69.2, 81.1, 124.3, 125.1, 125.8, 126.1, 126.3, 128.5, 129.0, 132.6, 133.8, 133.9, 169.2; IR (NaCl) 3051, 2973, 2927, 2852, 1737, 1515, 1455, 1370, 1261, 1192, 1106, 986 cm^{-1} ; MS (EI) m/z 258 (M^+).

Anal. Calcd for $\text{C}_{16}\text{H}_{18}\text{O}_3$: C, 77.41; H, 6.97; O, 18.60. Found: C, 77.44; H, 6.99; O, 18.63.

(\pm)-tert-Butyl α -O-Methyl- α -(1-naphthyl)acetate (6). A 41 mg portion of 6 was obtained from 50 mg of 16 and 17 mg of 2-methyl-2-propanol (85% yield): ^1H NMR (250.13 MHz, $\text{CS}_2 + \text{Cl}_2\text{CD}_2$) δ (ppm) 1.38 (s, 9H), 3.45 (s, 3H), 5.20 (s, 1H), 7.45–7.83 (m, 7 H); ^{13}C NMR (62.83 MHz, $\text{CS}_2 + \text{Cl}_2\text{CD}_2$ 4:1) δ (ppm) 28.5, 56.8, 80.7, 81.2, 124.4, 125.1, 125.2, 126.0, 126.1, 126.2, 128.8, 132.9, 133.7, 168.9; IR (NaCl) 3057, 2980, 2932, 2835, 2119, 1739, 1598, 1461, 1360, 1247, 1157, 990, 852 cm^{-1} ; MS (EI) m/z 272 (M^+).

Anal. Calcd for $\text{C}_{17}\text{H}_{20}\text{O}_3$: C, 75; H, 7.35; O, 17.64. Found: C, 75.03; H, 7.37; O, 17.68.

Acknowledgment. This work was financially supported by the CICYT (SAF 92–1023) and the Xunta de Galicia (XUGA 20907B/93). One of us (Sh.L.) acknowledges the Spanish Ministry for Education and Science for postdoctoral research grant.

Supplementary Material Available: Spectra of obtained compounds (20 pages). This material is contained in libraries on microfiche, immediately follows this article in the microfilm version of the journal, and can be ordered from the ACS; see any current masthead page for ordering information.

JO9415059